Testing for dynamical dark energy models with redshift-space distortions

JCAP01(2013)030

(http://iopscience.iop.org/1475-7516/2013/01/030)

Journal of Cosmology and Astroparticle Physics
An IOP and SISSA journal

Testing for dynamical dark energy models with redshift-space distortions

Shinji Tsujikawa,[a] **Antonio De Felice**[b,c] **and Jailson Alcaniz**[d]

[a]Department of Physics, Faculty of Science, Tokyo University of Science, 1-3, Kagurazaka, Shinjuku-ku, Tokyo 162-8601, Japan
[b]ThEP's CRL, NEP, The Institute for Fundamental Study, Naresuan University, Phitsanulok 65000, Thailand
[c]Thailand Center of Excellence in Physics, Ministry of Education, Bangkok 10400, Thailand
[d]Departamento de Astronomia, Observatório Nacional, 20921-400 Rio de Janeiro - RJ, Brasil

E-mail: shinji@rs.kagu.tus.ac.jp, antoniod@nu.ac.th, alcaniz@on.br

Received October 16, 2012
Revised December 12, 2012
Accepted December 30, 2012
Published January 24, 2013

Abstract. The red-shift space distortions in the galaxy power spectrum can be used to measure the growth rate of matter density perturbations δ_m. For dynamical dark energy models in General Relativity we provide a convenient analytic formula of $f(z)\sigma_8(z)$ written as a function of the redshift z, where $f = d\ln\delta_m/d\ln a$ (a is the cosmological scale factor) and σ_8 is the rms amplitude of over-density at the scale $8\,h^{-1}$ Mpc. Our formula can be applied to the models of imperfect fluids, quintessence, and k-essence, provided that the dark energy equation of state w does not vary significantly and that the sound speed is not much smaller than 1. We also place observational constraints on dark energy models of constant w and tracking quintessence from the recent data of red-shift space distortions.

Keywords: galaxy clustering, dark energy theory, modified gravity, gravity

doi:10.1088/1475-7516/2013/01/030

JCAP01(2013)030

Contents

1 Introduction

After the first discovery of cosmic acceleration from the distance measurements of the supernovae type Ia (SN Ia) [1], the existence of dark energy has been also supported from other observational data such as Cosmic Microwave Background (CMB) [2, 3] and Baryon Acoustic Oscillations (BAO) [4]. From the theoretical point of view, such a late-time cosmic acceleration is problematic because of the huge difference between the observed dark energy scale and the expected value of the vacuum energy appearing in particle physics [5]. Along with the cosmological constant Λ, many alternative acceleration mechanisms have been proposed, including modifications of the matter/energy content and large-scale modifications of gravity (see refs. [6, 7] for reviews).

The dark energy equation of state w is constrained by measuring the expansion rate of the Universe from the observations of SN Ia, CMB, and BAO [3, 8–11]. Although it is possible to rule out some accelerating scenarios from the analysis of the cosmic expansion history alone, we require further precise observational data to clearly distinguish between models with subtly-varying w. So far the Λ-Cold-Dark-Matter (ΛCDM) model has been consistent with the data, but there are many other dynamical models such as quintessence [12], k-essence [13, 14], and $f(R)$ gravity [15] which are compatible with current observations.

The large-scale structure of the galaxy distribution provides additional important information to discriminate between different dark energy models [16]. The galaxy clustering occurs due to the gravitational instability of primordial matter density perturbations. The growth rate of matter perturbations can be measured from the redshift-space distortion (RSD) of clustering pattern of galaxies. This distortion is caused by the peculiar velocity of

JCAP01(2013)030

inward collapse motion of the large-scale structure, which is directly related to the growth rate of the matter density contrast δ_m [17]. Hence the RSD measurement is very useful to constrain the cosmic growth history.

Recent galaxy redshift surveys have provided bounds on the growth rate $f(z)$ or $f(z)\sigma_8(z)$ in terms of the redshift $z = 1/a - 1$, where $f = d\ln\delta_m/d\ln a$ and σ_8 is the rms amplitude of δ_m at the comoving scale 8 h^{-1} Mpc (h is the normalized Hubble constant $H_0 = 100\,h\,\mathrm{km\,sec^{-1}\,Mpc^{-1}}$) [18–30]. Although the observational error bars of $f\sigma_8$ are not yet small, the data are consistent with the prediction of the ΛCDM model [24, 30]. Recently the RSD data were used to place constraints on modified gravity models such as $f(R)$ gravity and (extended) Galileons [31, 32]. Since the growth rate of matter perturbations in these models is different from that in the ΛCDM [33–35], the allowed parameter space is quite tightly constrained even from current observations.

For the models based on General Relativity (GR) without a direct coupling between dark energy and non-relativistic matter, the gravitational coupling appearing in the matter perturbation equation is equivalent to the Newton's gravitational constant, as long as the dark energy perturbation is negligible relative to the matter perturbation. Nonetheless the evolution of perturbations depends on the background cosmology, so that the dynamical dark energy models with w different from -1 can be distinguished from the ΛCDM. In particular, the future RSD observations may reach the level of discriminating between different dark energy models constructed in the framework of GR.

In this paper we derive an analytic formula of $f(z)\sigma_8(z)$ valid for dynamical dark energy models including imperfect fluids, quintessence, and k-essence. Provided that the sound speed c_s is not much smaller than 1 and that the variation of w is not significant, our formula can reproduce the full numerical solutions with high accuracy. The derivation of $f(z)\sigma_8(z)$ is based on the expansion of w in terms of the dark energy density parameter Ω_x, i.e., $w = w_0 + \sum_{n=1} w_n(\Omega_x)^n$. Since $f(z)\sigma_8(z)$ is expressed in terms of the present values of σ_8 and Ω_x as well as w_n ($n = 0, 1, 2, \cdots$), our formula is convenient to test for dynamical dark energy models with the observational data of the cosmic growth rate. For the models with constant w there are 3 parameters w_0, $\sigma_8(z=0)$, and $\Omega_x(z=0)$ in the analytic expression of $f(z)\sigma_8(z)$. In tracking quintessence models [36], where the dark energy equation of state is nearly constant during the matter era ($w = w_{(0)}$), we show that our formula of $f(z)\sigma_8(z)$ also contains only 3 parameters: $w_{(0)}$, $\sigma_8(z=0)$, and $\Omega_x(z=0)$. Using the recent RSD data, we carry out the likelihood analysis by varying these 3 parameters to find observational bounds on w_0 and $w_{(0)}$.

This paper is organized as follows. In section 2 we review cosmological perturbation theory in general dark energy models including imperfect fluids, quintessence, and k-essence. In section 3 dynamical dark energy models are classified depending on how the equation of state w is expanded in terms of Ω_x. In section 4 we derive an analytic formula for $f(z)\sigma_8(z)$ and in section 5 we confirm the validity of this formula in concrete examples of dark energy models. In section 6 we perform the likelihood analysis to test for constant w and tracking quintessence models with the recent RSD data. Section 7 is devoted to our main conclusions.

2 Cosmological perturbations and redshift-space distortions

As the dark energy component we consider a fluid characterized by the equation of state $w = P_x/\rho_x$, where P_x is the pressure and ρ_x is the energy density. We also take into account non-relativistic matter (cold dark matter and baryons) with the energy density ρ_m and treat

JCAP01(2013)030

it as a perfect fluid with the equation of state $w_m = 0$. We deal with such a two-fluid system in the framework of GR under the assumption that dark energy is uncoupled to non-relativistic matter. Our analysis covers quintessence [12] and k-essence [13, 14] models, in which the Lagrangian P of dark energy depends on a scalar field ϕ and a kinetic term $X = -(\nabla\phi)^2/2$. In these models we have that $P_x = P$ and $\rho_x = 2XP_{,X} - P$, where $P_{,X} \equiv \partial P/\partial X$.

In the flat Friedmann-Lemaître-Robertson-Walker (FLRW) background with the scale factor $a(t)$, where t is the cosmic time, dark energy and non-relativistic matter obey, respectively, the following continuity equations

$$\rho_x' + 3(1+w)\rho_x = 0\,, \tag{2.1}$$

$$\rho_m' + 3\rho_m = 0\,, \tag{2.2}$$

where a prime represents a derivative with respect to $N = \ln a$. We introduce the density parameters $\Omega_x = 8\pi G\rho_x/(3H^2)$ and $\Omega_m = 8\pi G\rho_m/(3H^2)$, where G is the gravitational constant and $H = \dot{a}/a$ is the Hubble parameter (a dot represents derivative with respect to t). From the Einstein equations it follows that

$$\Omega_x + \Omega_m = 1\,, \tag{2.3}$$

$$\frac{H'}{H} = -\frac{3}{2}(1 + w\Omega_x)\,. \tag{2.4}$$

The dark energy density parameter satisfies the differential equation

$$\Omega_x' = -3w\Omega_x(1 - \Omega_x)\,. \tag{2.5}$$

Let us consider scalar metric perturbations about the flat FLRW background. We neglect the contribution of tensor and vector perturbations. In the absence of the anisotropic stress the perturbed line element in the longitudinal gauge is given by [37]

$$ds^2 = -(1 - 2\Phi)\,dt^2 + a^2(t)(1 + 2\Phi)d\boldsymbol{x}^2\,, \tag{2.6}$$

where Φ is the gravitational potential. We decompose the energy densities ρ_i (where $i = x, m$) and the pressure P_x into the background and inhomogeneous parts, as $\rho_i = \rho_i(t) + \delta\rho_i(t, \boldsymbol{x})$ and $P_x = P_x(t) + \delta P_x(t, \boldsymbol{x})$. We also define the following quantities

$$\delta_i \equiv \frac{\delta\rho_i}{\rho_i}\,, \qquad \theta_i \equiv \frac{\nabla^2 v_i}{aH} \qquad (i = x, m), \tag{2.7}$$

where v_x and v_m are the rotational-free velocity potentials of dark energy and non-relativistic matter, respectively.

In Fourier space dark energy perturbations obey the following equations of motion [38–41]

$$\delta_x' + 3(c_x^2 - w)\delta_x = -(1+w)\left(3\Phi' + \theta_x\right)\,, \tag{2.8}$$

$$\theta_x' + \left(2 - 3w + \frac{H'}{H} + \frac{w'}{1+w}\right)\theta_x = \left(\frac{k}{aH}\right)^2\left(\frac{c_x^2}{1+w}\delta_x - \Phi\right)\,, \tag{2.9}$$

where $c_x^2 = \delta P_x/\delta\rho_x$ and k is a comoving wave number. The perturbed equations of non-relativistic matter (perfect fluids) are

$$\delta_m' = -3\Phi' - \theta_m\,, \tag{2.10}$$

$$\theta_m' + \left(2 + \frac{H'}{H}\right)\theta_m = -\left(\frac{k}{aH}\right)^2\Phi\,. \tag{2.11}$$

JCAP01(2013)030

From the Einstein equations we obtain

$$\left(\frac{k}{aH}\right)^2 \Phi = \frac{3}{2}\left(\Omega_m \hat{\delta}_m + \Omega_x \hat{\delta}_x\right) , \tag{2.12}$$

$$\Phi' + \Phi = -\frac{3}{2}\left(\frac{aH}{k}\right)^2 \left[\Omega_m \theta_m + (1+w)\Omega_x \theta_x\right] , \tag{2.13}$$

where $\hat{\delta}_m$ and $\hat{\delta}_x$ are the rest frame gauge-invariant density perturbations defined by

$$\hat{\delta}_m = \delta_m + 3\left(\frac{aH}{k}\right)^2 \theta_m , \qquad \hat{\delta}_x = \delta_x + 3\left(\frac{aH}{k}\right)^2 (1+w)\theta_x . \tag{2.14}$$

For imperfect fluids such as quintessence and k-essence there exist non-adiabatic entropy perturbations generated from dissipative processes. We introduce a gauge-invariant entropy perturbation δs_x of dark energy, as [38, 39, 42]

$$\delta s_x = (c_x^2 - c_a^2)\delta_x = \frac{\dot{P}_x}{\rho_x}\left(\frac{\delta P_x}{\dot{P}_x} - \frac{\delta \rho_x}{\dot{\rho}_x}\right) , \tag{2.15}$$

where c_a is the adiabatic sound speed defined by

$$c_a^2 = \frac{\dot{P}_x}{\dot{\rho}_x} = w - \frac{w'}{3(1+w)} . \tag{2.16}$$

In the rest frame where the entropy perturbation is given by $\delta s_x = (\hat{c}_x^2 - c_a^2)\hat{\delta}_x$, the sound speed squared $c_s^2 \equiv \hat{c}_x^2$ is gauge-invariant. Using the definition of $\hat{\delta}_x$ in eq. (2.14), the pressure perturbation of dark energy can be expressed as

$$\delta P_x = c_s^2 \, \delta \rho_x + 3\left(\frac{aH}{k}\right)^2 (1+w)(c_s^2 - c_a^2)\rho_x \theta_x , \tag{2.17}$$

whereas the sound speed squared $c_x^2 = \delta P_x / \delta \rho_x$ in the random frame is related to c_s^2 via

$$c_x^2 = c_s^2 + 3\left(\frac{aH}{k}\right)^2 (1+w)(c_s^2 - c_a^2)\frac{\theta_x}{\delta_x} . \tag{2.18}$$

In terms of c_s^2, eqs. (2.8) and (2.9) can be written as

$$\delta_x' + 3(c_s^2 - w)\delta_x = -3(1+w)\Phi' - (1+w)\left[1 + 9\left(\frac{aH}{k}\right)^2 (c_s^2 - c_a^2)\right]\theta_x , \tag{2.19}$$

$$\theta_x' + \left(2 + \frac{H'}{H} - 3c_s^2\right)\theta_x = \left(\frac{k}{aH}\right)^2 \left(\frac{c_s^2}{1+w}\delta_x - \Phi\right) . \tag{2.20}$$

In k-essence characterized by the Lagrangian density $P(\phi, X)$, the perturbed quantities can be expressed as

$$\delta \rho_x = \left(P_{,X} + 2X P_{,XX}\right)\delta X - \left(P_{,\phi} - 2X P_{,X\phi}\right)\delta \phi , \tag{2.21}$$

$$\delta P_x = P_{,X}\delta X + P_{,\phi}\delta \phi , \tag{2.22}$$

$$\theta_x = \frac{k^2}{a\dot{\phi}}\delta \phi , \tag{2.23}$$

JCAP01(2013)030

z	$f\sigma_8$	survey
0.067	0.423± 0.055	6dFGRS (2012) [27]
0.17	0.51± 0.06	2dFGRS (2004) [19]
0.22	0.42± 0.07	WiggleZ (2011) [24]
0.25	0.3512± 0.0583	SDSS LRG (2011) [25]
0.37	0.4602± 0.0378	SDSS LRG (2011) [25]
0.41	0.45± 0.04	WiggleZ (2011) [24]
0.57	0.415± 0.034	BOSS CMASS (2012) [26]
0.6	0.43± 0.04	WiggleZ (2011) [24]
0.78	0.38± 0.04	WiggleZ (2011) [24]

Table 1. Data of $f\sigma_8$ versus the redshift z measured from the RSD.

where $\delta\phi$ is the field perturbation and $\delta X = \dot{\phi}\,\dot{\delta\phi} + \dot{\phi}^2\Phi$. From eq. (2.17) the rest frame sound speed can be obtained by setting $\delta\phi = 0$ in eqs. (2.21) and (2.22), i.e., $c_s^2 = P_{,X}/(P_{,X} + 2XP_{,XX})$ [43]. In quintessence characterized by the Lagrangian $P = X - V(\phi)$, the sound speed squared reduces to $c_s^2 = 1$.

From eqs. (2.10) and (2.11) it follows that

$$\delta_m'' + \left(2 + \frac{H'}{H}\right)\delta_m' - \left(\frac{k}{aH}\right)^2 \Phi = -3\left[\Phi'' + \left(2 + \frac{H'}{H}\right)\Phi'\right]. \tag{2.24}$$

For the perturbations deep inside the Hubble radius ($k \gg aH$) relevant to large-scale structures, the r.h.s. of eq. (2.24) can be neglected relative to the l.h.s. of it, in addition to the fact that $\hat{\delta}_m \simeq \delta_m$. If the contribution of dark energy perturbations can be neglected relative to that of matter perturbations in eq. (2.12), i.e. $|\Omega_m\hat{\delta}_m| \gg |\Omega_x\hat{\delta}_x|$, eq. (2.24) reads

$$\delta_m'' + \frac{1}{2}\left(1 - 3w\Omega_x\right)\delta_m' - \frac{3}{2}\Omega_m\delta_m \simeq 0\,, \tag{2.25}$$

where we made use of eq. (2.4).

During the deep matter era in which $\Omega_m \simeq 1$, there is a growing-mode solution $\delta_m = \delta_m' \propto a$ to eq. (2.25). In this regime eq. (2.12) tells us that $\Phi =$ constant and hence $\theta_m \simeq -\delta_m'$ from eq. (2.10). For the dark energy density contrast δ_x, it is natural to choose the adiabatic initial condition [38, 41]

$$\delta_x = (1 + w)\delta_m\,. \tag{2.26}$$

The initial condition of θ_x is known by substituting eq. (2.26) and $\delta_x' = (1 + w + w')\delta_m$ into eq. (2.19). We will discuss the accuracy of the approximate equation (2.25) in section 3.

The growth rate of matter perturbations can be measured from the RSD in clustering pattern of galaxies because of radial peculiar velocities. The perturbation δ_g of galaxies is related to the matter perturbation δ_m, as $\delta_g = b\delta_m$, where b is a bias factor. The galaxy power spectrum $\mathcal{P}_g(\boldsymbol{k})$ in the redshift space can be expressed as [17, 44–46]

$$\mathcal{P}_g(\boldsymbol{k}) = \mathcal{P}_{gg}(\boldsymbol{k}) - 2\mu^2\mathcal{P}_{g\theta}(\boldsymbol{k}) + \mu^4\mathcal{P}_{\theta\theta}(\boldsymbol{k})\,, \tag{2.27}$$

where $\mu = \boldsymbol{k}\cdot\boldsymbol{r}/(kr)$ is the cosine of the angle of the $\boldsymbol{k}$ vector to the line of sight (vector $\boldsymbol{r}$), $\mathcal{P}_{gg}(\boldsymbol{k})$ and $\mathcal{P}_{\theta\theta}(\boldsymbol{k})$ are the real space power spectra of galaxies and θ, respectively, and $\mathcal{P}_{g\theta}(\boldsymbol{k})$ is the cross power spectrum of galaxy-θ fluctuations in real space.

JCAP01(2013)030

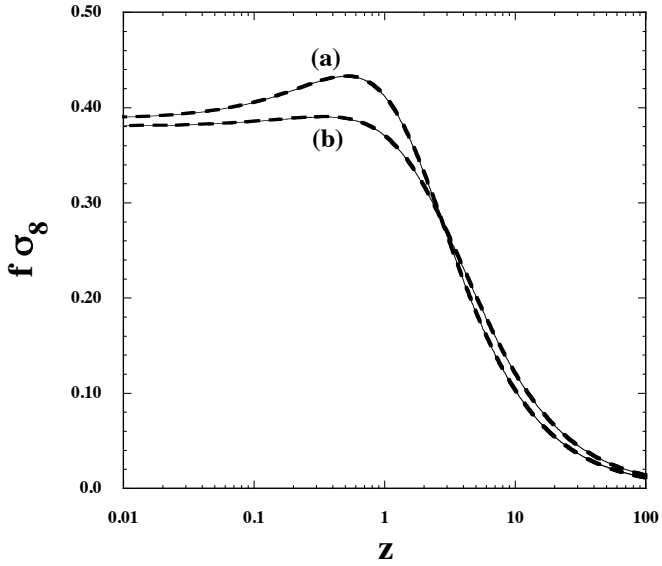

Figure 1. Evolution of $f\sigma_8$ versus the redshift z for $c_s^2 = 1$, $k = 0.07\,h$ Mpc^{-1}, $\sigma_8(z = 0) = 0.811$, and $\Omega_m(z = 0) = 0.73$. The cases (a) and (b) correspond to $w = -0.8$ and $w = -0.5$, respectively. The solid lines show the numerically integrated solutions, whereas the bald dashed lines correspond to the solutions derived by using the approximate equation (2.25).

In eq. (2.10) the variation of the gravitational potential is neglected relative to the growth rate of δ_m, so that

$$\theta_m \simeq -f\delta_m\,, \qquad f \equiv \frac{\dot{\delta}_m}{H\delta_m}\,. \tag{2.28}$$

Under the continuity equation (2.28), $\mathcal{P}_{gg}$, $\mathcal{P}_{g\theta}$, and $\mathcal{P}_{\theta\theta}$ in eq. (2.27) depend on $(b\delta_m)^2$, $(b\delta_m)(f\delta_m)$, and $(f\delta_m)^2$, respectively. We normalize the amplitude of δ_m at the scale $8\,h^{-1}$ Mpc, for which we write σ_8. Assuming that the growth of perturbations is scale-independent, the constraints on $b\delta_m$ and $f\delta_m$ translate into those on $b\sigma_8$ and $f\sigma_8$. The advantage of using $f\sigma_8$ is that the growth rate is directly known without the bias factor b. In table 1 we show the current data of $f\sigma_8$ as a function of z from the RSD measurements.

3 Dynamical dark energy models

In this section, we discuss a number of dynamical dark energy models in which the field equations presented in the previous section can be applied.

3.1 Imperfect fluids

For imperfect fluids the rest frame sound speed c_s is generally different from the adiabatic sound speed c_a. For constant w one has $c_a^2 = w$. If c_s^2 is constant as well, the evolution of dark energy perturbations is known by solving eqs. (2.19) and (2.20) together with the background equations (2.3)–(2.5). This is the approach taken in ref. [39]. Note also that for c_s of the order of 1 the contribution of dark energy perturbations to Φ in eq. (2.12) is negligibly small relative to matter perturbations [39, 47].

In figure 1 we plot the evolution of $f\sigma_8$ for $c_s^2 = 1$ and $k = 0.07\,h$ Mpc^{-1} with two different values of w. The approximate equation (2.25) reproduces the full numerical solution

within the 0.1 % accuracy. This means that, for $c_s^2 = 1$, the contribution of dark energy perturbations to the gravitational potential is suppressed relative to that of matter perturbations. For $c_s^2 = 0$ and $w = -0.8$ we find that the difference of $f\sigma_8(z = 0)$ between the numerical result and the approximated solution is about 4 % for the mode $k = 0.07\,h$ Mpc^{-1}. For w larger than -0.8 the difference gets even larger, but such values of w are not allowed observationally [3, 8]. In ref. [40] it was found that galaxy redshift and tomographic redshift surveys can constrain the sound speed only if c_s^2 is sufficiently small, of the order of $c_s^2 \lesssim 10^{-4}$.

3.2 Quintessence

Quintessence [12] is characterized by the Lagrangian $P(\phi, X) = X - V(\phi)$, where $V(\phi)$ is the field potential. In this case the sound speed c_s is equivalent to 1, so that the contribution of dark energy perturbations to the gravitational potential is negligible. There are several classes of potentials which give rise to different evolution of w.

The first class is the model with constant w, which can be realized by the following potential [6, 48, 49]

$$V(\phi) = \frac{3H_0^2(1-w)(1-\Omega_{m0})^{1/|w|}}{16\pi G\Omega_{m0}^{\alpha}} \sinh^{-2\alpha}\left(|w|\sqrt{\frac{6\pi G}{1+w}}(\phi - \phi_0 + \phi_1)\right), \tag{3.1}$$

where $\alpha = (1+w)/|w|$, ϕ_0 and Ω_{m0} are the today's values of ϕ and Ω_m respectively, and

$$\phi_1 = \sqrt{\frac{1+w}{6\pi G}}\frac{1}{|w|}\ln\frac{1+\sqrt{1-\Omega_{m0}}}{\sqrt{\Omega_{m0}}}\,. \tag{3.2}$$

This case is identified as an imperfect fluid with $c_s^2 = 1$ and $w =$ constant discussed in section 3.1.

The second class consists of freezing models [50], in which the evolution of the field gradually slows down at late times. A typical example is the inverse power-law potential [51]

$$V(\phi) = M^{4+p}\phi^{-p}\,, \tag{3.3}$$

where p is a positive constant. For this potential there exists a so-called tracker solution [36] with a nearly constant field equation of state $w = w_{(0)} \equiv -2/(p+2)$ during the matter era, which is followed by the decrease of w. Considering a homogeneous perturbation δw around $w_{(0)}$, the field equation of state is expressed as [52]

$$w = w_{(0)} + \sum_{n=1}^{\infty}\frac{(-1)^{n-1}w_{(0)}(1-w_{(0)}^2)}{1-(n+1)w_{(0)}+2n(n+1)w_{(0)}^2}\left(\frac{\Omega_x}{1-\Omega_x}\right)^n. \tag{3.4}$$

Expansion of w around Ω_x reads

$$\begin{aligned} w = w_{(0)} &+ \frac{(1-w_{(0)}^2)w_{(0)}}{1-2w_{(0)}+4w_{(0)}^2}\Omega_x + \frac{(1-w_{(0)}^2)w_{(0)}^2(8w_{(0)}-1)}{(1-2w_{(0)}+4w_{(0)}^2)(1-3w_{(0)}+12w_{(0)}^2)}\Omega_x^2 \\ &+ \frac{2(1-w_{(0)}^2)w_{(0)}^3(4w_{(0)}-1)(18w_{(0)}+1)}{(1-2w_{(0)}+4w_{(0)}^2)(1-3w_{(0)}+12w_{(0)}^2)(1-4w_{(0)}+24w_{(0)}^2)}\Omega_x^3 + \mathcal{O}(\Omega_x^4)\,, \end{aligned} \tag{3.5}$$

which varies with the growth of Ω_x.

JCAP01(2013)030

The third class consists of thawing models [50], in which the field is nearly frozen by a Hubble friction during the early cosmological epoch and it starts to evolve once the field mass m drops below H. In this case w is initially close to -1 and then w starts to grow at late times. The representative potential of this class is that of the pseudo Nambu-Goldstone boson [53], i.e.,

$$V(\phi) = \Lambda^4 \left[1 + \cos(\phi/f)\right] , \tag{3.6}$$

where Λ and f are constants. Assuming that the evolution of the scale factor can be approximated as that of the ΛCDM model, the field equation of state is estimated as [54] (see also ref. [55])

$$w = -1 + (1+\tilde{w}_0) a^{3(K-1)} \left[\frac{(K - F(a))(F(a)+1)^K + (K + F(a))(F(a)-1)^K}{(K - \Omega_{x0}^{-1/2})(\Omega_{x0}^{-1/2}+1)^K + (K + \Omega_{x0}^{-1/2})(\Omega_{x0}^{-1/2}-1)^K} \right]^2 , \tag{3.7}$$

where $\tilde{w}_0$ and Ω_{x0} are the today's values of w and Ω_x respectively, and

$$K = \sqrt{1 - \frac{V_{,\phi\phi}(\phi_i)}{6\pi G V(\phi_i)}} , \qquad F(a) = \sqrt{1 + (\Omega_{x0}^{-1} - 1) a^{-3}} . \tag{3.8}$$

The constant K is related to the mass of the field at the initial displacement, $\phi = \phi_i$. Expansion around $\Omega_x = 0$ gives

$$w = -1 + w_1 \Omega_x + \frac{1}{5}(K^2+1) w_1 \Omega_x^2 + \frac{1}{175}(3K^4 + 31K^2 + 3) w_1 \Omega_x^3 + \mathcal{O}(\Omega_x^4) , \tag{3.9}$$

where

$$w_1 = \frac{4}{9} \frac{1 + \tilde{w}_0}{[(K - \Omega_{x0}^{-1/2})(\Omega_{x0}^{-1/2}+1)^K + (K + \Omega_{x0}^{-1/2})(\Omega_{x0}^{-1/2}-1)^K]^2} \times \left(\frac{1 - \Omega_{x0}}{\Omega_{x0}} \right)^{K-1} K^2 (K-1)^2 (K+1)^2 . \tag{3.10}$$

The growth of Ω_x leads to the deviation from $w = -1$.

3.3 K-essence

The equation of state for K-essence with the Lagrangian density $P(\phi, X)$ is given by $w = P/(2XP_{,X} - P)$. This shows that cosmic acceleration with $w \approx -1$ can be realized either for (a) $X \approx 0$ or (b) $P_{,X} \approx 0$.

In the case (a) Chiba et al. [56] showed that, for the factorized function $P(\phi, X) = V(\phi)F(X)$, the field equation of state is given by the same form as eq. (3.7) with the replacement $K = \sqrt{1 - V_{,\phi\phi}(\phi_i)/(6\pi G F_{,X}(0) V^2(\phi_i))}$, where $F(X)$ is expanded around $X = 0$ as $F(X) = F(0) + F_{,X}(0)X$. In this case the sound speed squared is also close to 1, so that the situation is similar to that in thawing quintessence models.

In the case (b) the evolution of w depends on the functional form of $P(\phi, X)$, so it is difficult to derive a general expression of w [56]. One of the examples which belongs to this class is the dilatonic ghost condensate model [57] characterized by the Lagrangian $P(\phi, X) = -X + e^{\kappa\lambda\phi} X^2/M^4$, where $\kappa = \sqrt{8\pi G}$, λ and M are constants (see also ref. [58]). In this model the fixed points during the radiation and matter eras correspond to $P_{,X} = 0$ and $w = -1$, i.e., $y \equiv X e^{\kappa\lambda\phi}/M^4 = 1/2$. On the other hand the (no-ghost) accelerated fixed point corresponds

JCAP01(2013)030

to $y = 1/2+\lambda^2 f(\lambda)/16$ with the equation of state $w = -[1-\lambda^2 f(\lambda)/8]/[1+3\lambda^2 f(\lambda)/8] > -1$, where $f(\lambda) = 1 + \sqrt{1+16/(3\lambda^2)}$. Hence the evolution of w is similar to that in thawing quintessence models.

The sound speed squared in the dilatonic ghost condensate model is given by $c_s^2 = (2y-1)/(6y-1)$, so that $c_s^2 \simeq 0$ during radiation and matter eras. The late-time cosmic acceleration occurs for $1/2 \leq y < 2/3$ and hence $0 \leq c_s^2 < 1/9$ at this fixed point. The fact that c_s^2 is close to 0 during most of the cosmological epoch is a different signature relative to quintessence. However, since w is very close to -1 during radiation and matter eras, the adiabatic initial condition (2.26) shows that the dark energy perturbation δ_x is initially suppressed relative to the matter perturbation δ_m. As long as the today's value of w is not significantly away from -1 the contribution of the dark energy perturbation to Φ is suppressed relative to the matter perturbation, so that the approximate equation (2.25) can be trustable even in such cases.

4 Analytic solutions of $f\sigma_8$

We derive analytic solutions of $f\sigma_8$ by solving the approximate equation (2.25). Recall that the equation of state for tracking and thawing models of quintessence can be expressed in terms of the field density parameter Ω_x, see eqs. (3.5) and (3.9). We generally expand the dark energy equation of state in terms of the density parameter Ω_x, as

$$w = w_0 + \sum_{n=1}^{\infty} w_n (\Omega_x)^n \,. \tag{4.1}$$

Since Ω_x grows as large as 0.7 today, we expect that it may be necessary to pick up the terms higher than the first few terms in eq. (4.1).

In terms of the function $f = \delta_m'/\delta_m$, eq. (2.25) can be written as [59]

$$3w\Omega_x(1-\Omega_x)\frac{df}{d\Omega_x} = f^2 + \frac{1}{2}(1-3w\Omega_x)f - \frac{3}{2}(1-\Omega_x)\,, \tag{4.2}$$

where we employed eq. (2.5). Introducing the growth index γ as $f = (\Omega_m)^\gamma = (1-\Omega_x)^\gamma$ [60], eq. (4.2) reads

$$3w\Omega_x(1-\Omega_x)\ln(1-\Omega_x)\frac{d\gamma}{d\Omega_x} = \frac{1}{2} - \frac{3}{2}w(1-2\gamma)\Omega_x + (1-\Omega_x)^\gamma - \frac{3}{2}(1-\Omega_x)^{1-\gamma}\,. \tag{4.3}$$

We derive the solution of eq. (4.3) by expanding γ in terms of Ω_x, i.e., $\gamma = \gamma_0 + \sum_{n=1}\gamma_n(\Omega_x)^n$. While Ω_m is smaller than Ω_x today, the former is not suitable as an expansion parameter as we would like to derive an analytic formula valid at high redshifts as well. In fact, it is expected that future RSD surveys such as Subaru/FMOS will provide high-redshift data up to $z = 2$. Using the expansion of w in eq. (4.1) as well, we obtain the following approximate solution

$$\begin{aligned}\gamma = {} & \frac{3(1-w_0)}{5-6w_0} + \frac{3}{2}\frac{(1-w_0)(2-3w_0)+2w_1(5-6w_0)}{(5-6w_0)^2(5-12w_0)}\Omega_x \\ & +[(w_0-1)(3w_0-2)(324w_0^2-420w_0+97)+12(5-6w_0)^2(5w_2-12w_2w_0+12w_1^2) \\ & +6(5-6w_0)(72w_0^2-90w_0+23)w_1]/[4(5-6w_0)^3(5-12w_0)(5-18w_0)]\,\Omega_x^2 \\ & +\mathcal{O}(\Omega_x^3)\,. \end{aligned} \tag{4.4}$$

The 1-st order solution is identical to the one found in ref. [61] by setting $w_1 = 0$. For $w_0 = -1$, $w_1 = 0$, and $w_2 = 0$ it follows that $\gamma \simeq 0.545 + 7.29 \times 10^{-3}\Omega_x + 4.04 \times 10^{-3}\Omega_x^2$. In this case the second and third terms are indeed much smaller than the first one, so that γ is nearly constant. For the models with $w_0 = -1$, $w_1 = 0.3$, and $w_2 = 0$ (in which case the value of w today is around -0.8) one has $\gamma \simeq 0.545 + 1.21 \times 10^{-2}\Omega_x + 6.55 \times 10^{-3}\Omega_x^2$. Even in this case the variation of γ induced by the second and third terms is small (see also refs. [62] for related works).

From the definition of f the matter perturbation obeys the differential equation $(\ln \delta_m)' = (1 - \Omega_x)^\gamma$. Using eq. (2.5), we obtain

$$\frac{d}{d\Omega_x} \ln \delta_m = -\frac{(1-\Omega_x)^{\gamma-1}}{3w\Omega_x} \,. \tag{4.5}$$

In the following we derive the solution of this equation under the approximation that γ is constant. We expand the term $(1 - \Omega_x)^{\gamma-1}$ around $\Omega_x = 0$, as

$$(1-\Omega_x)^{\gamma-1} = 1 + \sum_{n=1}^{\infty} \alpha_n (\Omega_x)^n \,, \qquad \alpha_n = \frac{(-1)^n}{n!}(\gamma-1)(\gamma-2)\cdots(\gamma-n) \,. \tag{4.6}$$

In order to evaluate the r.h.s. of eq. (4.5), we expand $1/w$ in the form

$$\frac{1}{w} = \frac{1}{w_0}\left[1 + \sum_{n=1}^{\infty} \beta_n (\Omega_x)^n\right] \,, \tag{4.7}$$

where the coefficients β_n's can be expressed by w_n's, say $\beta_1 = -w_1/w_0$. Then eq. (4.5) can be written as

$$\frac{d}{d\Omega_x} \ln \delta_m = -\frac{1}{3w_0\Omega_x}\left[1 + \sum_{n=1}^{\infty} c_n (\Omega_x)^n\right] \,, \tag{4.8}$$

where

$$c_n = \sum_{i=0}^{n} \alpha_{n-i}\beta_i \,, \tag{4.9}$$

with $\alpha_0 = \beta_0 = 1$. The first three coefficients c_i are

$$c_1 = -(\gamma-1) - \frac{w_1}{w_0} \,, \tag{4.10}$$

$$c_2 = \frac{1}{2}(\gamma-1)(\gamma-2) + (\gamma-1)\frac{w_1}{w_0} - \frac{w_2 w_0 - w_1^2}{w_0^2} \,, \tag{4.11}$$

$$\begin{aligned} c_3 = {} & -\frac{1}{6}(\gamma-1)(\gamma-2)(\gamma-3) - \frac{1}{2}(\gamma-1)(\gamma-2)\frac{w_1}{w_0} \\ & + (\gamma-1)\frac{w_2 w_0 - w_1^2}{w_0^2} - \frac{w_3 w_0^2 - 2w_1 w_2 w_0 + w_1^3}{w_0^3} \,. \end{aligned} \tag{4.12}$$

Integrating eq. (4.8), it follows that

$$\delta_m = \delta_{m0} \exp\left\{\frac{1}{3w_0}\left[\ln\frac{\Omega_{x0}}{\Omega_x} + \sum_{n=1}^{\infty}\frac{c_n}{n}\left((\Omega_{x0})^n - (\Omega_x)^n\right)\right]\right\} \,, \tag{4.13}$$

JCAP01(2013)030

where δ_{m0} is the today's value of δ_m. Normalizing δ_{m0} in terms of $\sigma_8(z=0)$, we obtain the following expression

$$f\sigma_8(z) = (1-\Omega_x)^\gamma\,\sigma_8(z=0)\,\exp\left\{\frac{1}{3w_0}\left[\ln\frac{\Omega_{x0}}{\Omega_x}+\sum_{n=1}^{\infty}\frac{c_n}{n}\left((\Omega_{x0})^n-(\Omega_x)^n\right)\right]\right\}. \qquad (4.14)$$

In terms of the redshift z the energy densities of non-relativistic matter and dark energy are given, respectively, by $\rho_m = \rho_{m0}(1+z)^3$ and $\rho_x = \rho_{x0}\exp[\int_0^z 3(1+w)/(1+\tilde{z})d\tilde{z}]$. The 0-th order solution to the field energy density is obtained by substituting $w = w_0$ into the expression of ρ_x, i.e., $\rho_x^{(0)} = \rho_{x0}(1+z)^{3(1+w_0)}$. This gives the 0-th order solution to Ω_x, as $\Omega_x^{(0)} = \Omega_{x0}(1+z)^{3w_0}/[1-\Omega_{x0}+\Omega_{x0}(1+z)^{3w_0}]$. If we expand w up to first order with respect to Ω_x, we can use the iterative solution $w = w_0 + w_1\Omega_x^{(0)}$. This process leads to the following integrated solution of Ω_x:

$$\Omega_x^{(1)} = \frac{\Omega_{x0}(1+z)^{3w_0}[1-\Omega_{x0}+\Omega_{x0}(1+z)^{3w_0}]^{w_1/w_0}}{1-\Omega_{x0}+\Omega_{x0}(1+z)^{3w_0}[1-\Omega_{x0}+\Omega_{x0}(1+z)^{3w_0}]^{w_1/w_0}}. \qquad (4.15)$$

In the presence of the terms higher than second order, we can simply carry out the similar iterative processes. Practically it is sufficient to use the 1-st order solution (4.15) for the evaluation of Ω_x in eq. (4.14).

The growth factor γ in eq. (4.14) is given by the analytic formula (4.4). Since γ is expressed in terms of w_n $(n = 0, 1, \cdots)$ and Ω_x, this means that $f\sigma_8(z)$ depends on the free parameters w_i, Ω_{x0}, and $\sigma_8(z=0)$. For the models of constant equation of state there are 3 free parameters w_0, Ω_{x0}, $\sigma_8(z=0)$ in the expression of $f\sigma_8(z)$.

In tracking quintessence models the coefficients w_n's $(n \geq 1)$ are expressed in terms of $w_0 = w_{(0)}$, see eq. (3.5). Hence there are only 3 free parameters w_0, Ω_{x0}, and $\sigma_8(z=0)$. In thawing models of quintessence one has $w_0 = -1$ and w_n's $(n \geq 2)$ can be expressed in terms of w_1 and K, see eqs. (3.9). Then $f\sigma_8$ in eq. (4.14) is written as a function of z with 4 free parameters: w_1, Ω_{x0}, $\sigma_8(z=0)$, and K.

5 Validity of analytic solutions

We study the validity of the analytic estimation given in the previous section. We discuss three different cases: (i) constant w models, (ii) tracking models, and (iii) thawing models, separately. In all the numerical simulations in this section, we identify the present epoch to be $\Omega_{x0} = 0.73$ with $\sigma_8(z=0) = 0.811$.

5.1 Constant w models

Let us first study constant w models realized by either imperfect fluids or quintessence. Unless $c_s^2 \ll 1$ the dark energy perturbation is negligible relative to the matter perturbation, so that the approximate equation (2.25) is sufficiently accurate. Since $w_n = 0$ $(n \geq 1)$, the coefficients c_n and Ω_x are given, respectively, by

$$c_n = \alpha_n = \frac{(-1)^n}{n!}(\gamma-1)(\gamma-2)\cdots(\gamma-n), \qquad \Omega_x = \frac{\Omega_{x0}(1+z)^{3w_0}}{1-\Omega_{x0}+\Omega_{x0}(1+z)^{3w_0}}. \qquad (5.1)$$

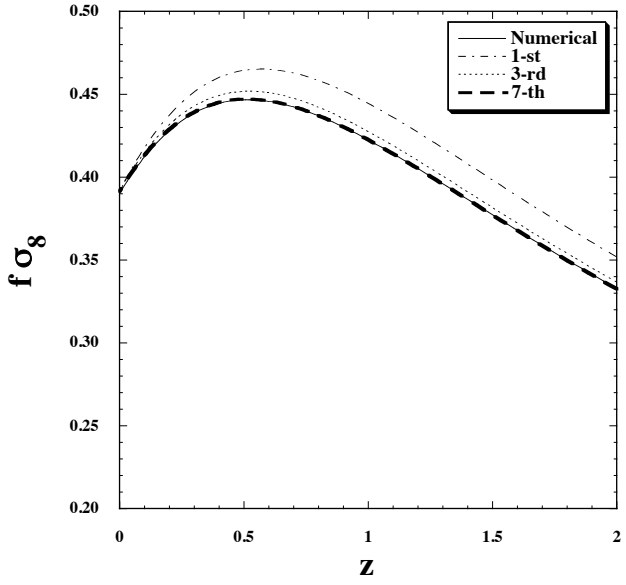

Figure 2. Evolution of $f\sigma_8$ versus z for the constant w model with $w = -0.9$ and $c_s^2 = 1$. The present epoch is identified to be $\Omega_{x0} = 0.73$ with $\sigma_8(z = 0) = 0.811$. The solid line shows the numerically integrated solution, whereas the dot-dashed, dotted, and bold dashed lines correspond to the solutions summed up to 1-st, 3-rd, and 7-th order terms of c_n in eq. (4.14).

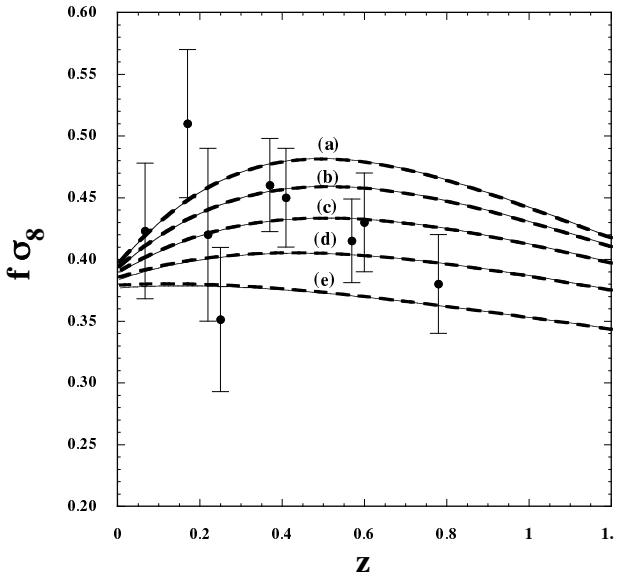

Figure 3. Evolution of $f\sigma_8$ versus z for the models with $c_s^2 = 1$ and (a) $w = -1.2$, (b) $w = -1$, (c) $w = -0.8$, (d) $w = -0.6$, (e) $w = -0.4$, respectively. The solid lines correspond to the numerically integrated solutions, whereas the bald dashed lines are derived from the analytic estimation (4.14) with the 10-th order terms of c_n. We also show the current RSD data.

For the growth index (4.4) we take into account the terms up to 2-nd order with respect to Ω_x, i.e.,

$$\gamma = \frac{3(1-w_0)}{5-6w_0} + \frac{3}{2}\frac{(1-w_0)(2-3w_0)}{(5-6w_0)^2(5-12w_0)}\Omega_x + \frac{(w_0-1)(3w_0-2)(324w_0^2-420w_0+97)}{4(5-6w_0)^3(5-12w_0)(5-18w_0)}\Omega_x^2 \,. \tag{5.2}$$

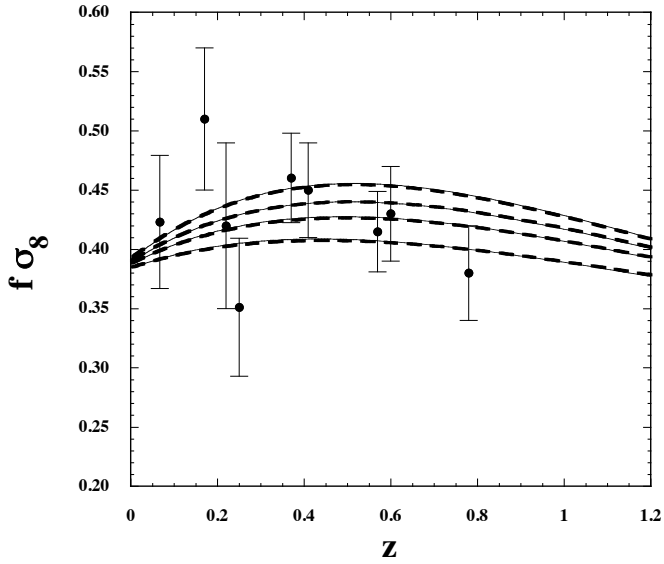

Figure 4. Evolution of $f\sigma_8$ versus z for the tracking quintessence model characterized by the inverse power-law potential $V(\phi) = M^{4+p}\phi^{-p}$. From top to bottom the solid lines correspond to the numerically integrated solutions for $p = 0.1, 0.5, 1, 2$, respectively, whereas the bold dashed lines are derived from the analytic solution (4.14) with the 10-th order terms. The RSD data are the same as those given in figure 3.

Recall that the terms higher than 2-nd order in γ are negligibly small. Then $f\sigma_8$ is analytically known from eq. (4.14) just by specifying the values of $\sigma_8(z = 0)$, Ω_{x0}, and $w = w_0$.

In figure 2 we plot the evolution of $f\sigma_8$ obtained by the analytic estimation (4.14) for $w = -0.9$ and $c_s^2 = 1$. A number of different lines correspond to the solutions derived by taking into account the c_n terms up to 1-st, 3-rd, and 7-th orders. As we pick up higher-order coefficients c_n in eq. (5.1), the solutions tend to approach the numerically integrated solution of $f\sigma_8$. In figure 2 we find that the solution up to 7-th order terms of c_n can reproduce the full numerical result in good precision.

In figure 3 we show $f\sigma_8$ versus z for five different values of w. In order to obtain a good convergence we pick up the c_n terms up to 10-th order. Figure 3 shows that our analytic estimation (4.14) is sufficiently trustable to reproduce the numerically integrated solutions accurately. If we only pick up the terms inside γ up to 1-st order with respect to Ω_x, there is small difference of $f\sigma_8$ between the analytic estimation and the numerical solutions for $w \gtrsim -0.6$ (which occurs in the low redshift regime). Taking into account the 2-nd order term in eq. (4.4), this difference gets smaller. Figure 3 also displays the RSD data given in table 1, which will be used to place observational constraints on w in section 6.

5.2 Tracking quintessence models

From eq. (3.5), we see that all coefficients w_n's ($n \geq 1$) in tracking models of quintessence are expressed in terms of the tracker equation of state $w_0 = w_{(0)}$. In this case there are contributions to c_n coming from the variation of w, i.e., non-zero values of β_n. Note that β_n's depend only on $w_{(0)}$.

For the tracking quintessence with the inverse power-law potential $V(\phi) = M^{4+p}\phi^{-p}$ ($p > 0$), we compare the numerically integrated solutions of $f\sigma_8$ with those derived by the analytic expression (4.14). In figure 4 we show the evolution of $f\sigma_8$ for $p = 0.1, 0.5, 1, 2$

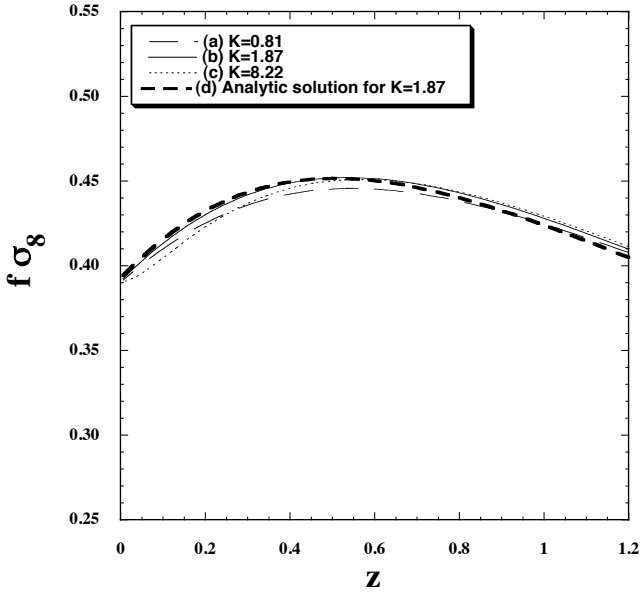

Figure 5. Evolution of $f\sigma_8$ versus z for the freezing quintessence with the potential $V(\phi) = \Lambda^4[1 + \cos(\phi/f)]$. The cases (a)-(c) correspond to the full numerical solutions with the model parameters (a) $K = 0.81$, $w_1 = 0.17$, (b) $K = 1.87$, $w_1 = 4.7 \times 10^{-2}$, and (c) $K = 8.22$, $w_1 = 3.6 \times 10^{-6}$, respectively, whereas the case (d) is derived by the 10-th order analytic solution (4.14) for $K = 1.87$, $w_1 = 4.7 \times 10^{-2}$.

evaluated from (4.14) as well as the numerical solutions. In eq. (4.14) we take into account the c_n's up to 10-th order terms, whereas in the analytic expression of γ in eq. (4.4) the terms up to 2-nd order in Ω_x are included. For the evaluation of Ω_x the 1-st order solution (4.15) with $\Omega_{x0} = 0.73$ is used. From figure 4 we find that the analytic solution (4.14) is accurate enough to reproduce the full numerical solution in high precisions. If we take into account the c_n's up to the 3-rd order terms, for example, there is some difference between the analytic and numerical results. This difference tends to disappear by including the higher-order terms of c_n. While the terms up to 10-th order are taken into account in figure 4, the 7-th order solutions are sufficiently accurate.

While our analytic formula of $f\sigma_8$ is trustable, readers may think that 7-th order expansion of c_n is not very convenient for practical purpose. However, using this analytic formula is simpler than solving the perturbation equations numerically for arbitrary initial conditions. If we take the latter approach, we need first to identify the present epoch (say, $0.7 < \Omega_{x0} < 0.73$) by solving the background equations from some redshift ($z = z_i$). Then the perturbation equations are solved with arbitrary initial values of $\sigma_8(z_i)$ to find $f\sigma(z)$ for each z. On the other hand, with our analytic formula, the likelihood analysis in terms of 3 free parameters w_0, $\sigma_8(z = 0)$, and Ω_{x0} can be done much easier even with the 7-th order expansion of c_n. We also would like to stress that our formula of $f\sigma_8(z)$ includes the free parameters $\sigma_8(z = 0)$ and Ω_{x0} *today*, by which the joint analysis with other data (such as CMB) can be conveniently performed.

5.3 Thawing models

In thawing models of quintessence the field equation of state is given by eq. (3.7). For larger K the deviation of w from -1 occurs at later times with a sharper transition. From eq. (3.9)

JCAP01(2013)030

we find that the higher-order terms in Ω_x are not negligible for K larger than the order of 1. In fact we have numerically confirmed that, for $K > \mathcal{O}(1)$, the expansion (3.9) does not accommodate the rapid transition of w at late times unless the higher-order terms are fully taken into account. This property also holds for the evolution of $f\sigma_8$. Only when K is smaller than the order of 1, the analytic estimation (4.14) can reproduce the full numerical solutions in good precision.

In figure 5 we plot the numerical evolution of $f\sigma_8$ for the potential $V(\phi) = \Lambda^4[1 + \cos(\phi/f)]$ with three different values of K. Since w is close to -1 in all these cases and the deviation from $w = -1$ occurs only at late times, the evolution of $f\sigma_8$ is not very different from each other for $K < 10$. From this analysis, it is clear that, only when very accurate data of $f\sigma_8$ are available in the future, it will be possible to distinguish between the models with different values of K. In figure 5 we also show the analytic solution derived for $K = 1.87$ and $w_1 = 4.7 \times 10^{-2}$ as the bold dashed line (d). We take into account the c_n's up to 10-th order to evaluate $f\sigma_8$ in eq. (4.14). Compared to the full numerical solution labelled as (b), there is a small difference in the high-redshift regime. We confirm that this deviation tends to be smaller by involving the c_n's higher than 10-th order. For $K < 1$ the analytic estimation is more accurate even without including such higher-order terms.

6 Constraints from the current RSD data

In this section, we place observational bounds on two models of dark energy discussed in sections 5.1 and 5.2 by using the current RSD data presented in table 1. For the today's value of σ_8 we consider the prior obtained from observations of CMB, BAO, and Hubble constant measurement (H_0), i.e.,

$$\sigma_8(z = 0) = 0.816 \pm 0.024\,. \tag{6.1}$$

Here and in what follows all the error bars correspond to the 68.3% confidence level (CL). Recall that we derived the analytic formula (4.14) under the approximation that the dark energy perturbation is neglected relative to the matter perturbation. For the validity of this approximation we put the prior $w < -0.1$.

6.1 Constant w models

For the models of constant w the today's matter density parameter constrained from SN Ia, CMB, BAO, and H_0 observations is [8]

$$\Omega_{m0} = 0.272^{+0.013}_{-0.013}\,. \tag{6.2}$$

Under the priors (6.1) and (6.2) we estimate the best-fit to the set of parameters $\mathbf{P} \equiv (w, \sigma_8(z = 0), \Omega_{m0})$ by evaluating the likelihood distribution function, $\mathcal{L} \propto e^{-\chi^2/2}$, with

$$\chi^2 = \sum_{i=1}^{9} \left(\frac{f\sigma_{8,\mathrm{ob}}(z_i) - f\sigma_{8,\mathrm{th}}(z_i)}{\sigma_i} \right)^2 . \tag{6.3}$$

Here $f\sigma_{8,\mathrm{ob}}(z_i)$ $(i = 1, \cdots, 9)$ are the 9 data displayed in table 1 with the error bars σ_i, whereas $f\sigma_{8,\mathrm{th}}(z_i)$ are the theoretical values derived from the analytic solution (4.14). For the evaluation of $f\sigma_{8,\mathrm{th}}(z_i)$ we pick up the c_n's up to 10-th order. For the growth index γ the terms up to 2-nd order with respect to Ω_x are included in eq. (4.4). For Ω_x we use the

JCAP01(2013)030

1-st order solution (4.15). In tracking quintessence models analyzed in section 6.2 we also take the same orders of expansions for $f\sigma_8$, γ, and Ω_x.

We find that the best-fit model parameters are

$$w = -0.604\,, \qquad \sigma_8(z=0) = 0.840\,, \qquad \Omega_{m0} = 0.285\,, \tag{6.4}$$

with reduced $\chi^2_r = 0.947$ ($\chi^2_r \equiv \chi^2_{\rm min}/\nu$, where ν stands for the degrees of freedom). At 68.3% CL, our analysis restricts the equation-of-state parameter to the interval

$$-1.245 < w < -0.347\,, \tag{6.5}$$

whereas $\sigma_8(z=0)$ and Ω_{m0} are unconstrained by current data even assuming the priors (6.1) and (6.2). Although the current bounds on w are weaker than those arising from background tests (see, e.g., refs. [3, 8]), we expect that upcoming RSD data from ongoing and planned galaxy redshift surveys can improve this situation in the near future.

6.2 Tracking quintessence models

For the tracking quintessence models in which the equation of state is given by eq. (3.4) we also carry out the likelihood analysis by using the analytic solution (4.14) of $f\sigma_8$ as well as the expressions for γ and Ω_x given in eqs. (4.4) and (4.15) respectively. While the equation of state (3.4) is derived for quintessence, we do not impose the prior $w_{(0)} > -1$ for generality. For this kind of models, a joint analysis involving current SN Ia, CMB, and BAO gives the following bound on the matter density parameter [63]:

$$0.273 < \Omega_{m0} < 0.293\,, \tag{6.6}$$

which is used in our analysis as a prior for Ω_{m0}. The best-fit model parameters are found to be

$$w_{(0)} = -0.461\,, \qquad \sigma_8(z=0) = 0.840\,, \qquad \Omega_{m0} = 0.293\,, \tag{6.7}$$

with $\chi^2_r = 0.923$. At 68.3% CL, we found

$$-1.288 < w_{(0)} < -0.214\,, \tag{6.8}$$

whereas the parameters $\sigma_8(z=0)$ and Ω_{m0} are again unconstrained in the regions of (6.1) and (6.6). As expected, the bounds on $w_{(0)}$ are weaker than those obtained in constant w models [eq. (6.5)]. We note that in tracking models the equation of state decreases at late times, which is accompanied by the decrease of $f\sigma_8$. Compared to constant w models, this allows the possibility to fit the data better even for larger values of w during the matter era.

7 Conclusions

In this paper we have provided an analytic formula of $f\sigma_8$ for dynamical dark energy models in the framework of GR. This was derived by using the approximate matter perturbation equation (2.25), which is trustable as long as the contribution of the dark energy perturbation to the gravitational potential is negligible relative to that of the matter perturbation. Our formula of $f\sigma_8$ can be applied to many dark energy models including imperfect fluids, quintessence, and k-essence in which the sound speed squared c_s^2 is not very close to 0.

Our derivation of $f\sigma_8$ is based on the expansion of w with respect to the dark energy density parameter Ω_x, i.e., $w = w_0 + \sum_{n=1} w_n (\Omega_x)^n$. The growth rate $f = \delta_m'/\delta_m$ of matter

JCAP01(2013)030

perturbations is parametrized by the growth index γ, as $f = (1-\Omega_x)^\gamma$. We expanded γ in terms of Ω_x up to 2-nd order terms. Since γ is dominated by the term $\gamma_0 = 3(1-w_0)/(5-6w_0)$, it is a good approximation to treat γ as a constant for the derivation of the integrated solution of δ_m. The c_n's in eq. (4.14) are given by eq. (4.9), where α_n and β_n appear as the coefficients of the expansion of the terms $(1-\Omega_x)^{\gamma-1}$ and $1/w$ respectively. For the density parameter Ω_x, the 1-st order solution (4.15) is usually sufficient to obtain accurate analytic solutions of $f\sigma_8$.

In section 5 we have studied the validity of the analytic formula (4.14) in concrete models of dark energy. For constant w models in which c_n and Ω_x are given by eq. (5.1), the analytic solution up to 7-th order terms of c_n reproduces the numerically integrated solutions with good precision. This property also holds for tracking quintessence models where the evolution of w is given by eq. (3.5). In thawing quintessence and k-essence models, where w is given by eq. (3.7), the formula (4.14) can be trustable for $K \lesssim 1$, but for K larger than the order of 1, we need to fully take into account the higher-order terms of c_n to have good convergence of $f\sigma_8$.

In section 6 we have discussed observational constraints on two different dark energy models by using the current RSD data. In both constant w and tracking quintessence models the analytic solution (4.14) includes the three parameters $\sigma_8(z=0)$, Ω_{m0}, and w (or $w_{(0)}$). Under the priors on $\sigma_8(z=0)$ and Ω_{m0} constrained by SN Ia, CMB, BAO, and H_0 measurements, we derived the bounds $-1.245 < w < -0.347$ (68 % CL) for constant w models and $-1.288 < w_{(0)} < -0.214$ (68 % CL) for tracking quintessence models. Although the upper bounds on the dark energy equation of state are still weak with current data, we expect to obtain more precise data from ongoing surveys or near-future projects such as Subaru/FMOS, HETDEX, and J-PAS. Our analytic formula of $f\sigma_8$ will be useful to place tighter bounds on dynamical dark energy models in the future.

So far, observational bounds on $f\sigma_8$ (listed in table 1) have been derived in the standard cosmological scenario without taking into account additional effects such as a possible coupling between dark matter and dark energy, irrotational flow, and so on. Reflecting this observational status, we did not assume any non-standard picture to estimate the theoretical values of $f\sigma_8$. However, if the standard cosmological scenario does not match with future high-precision data very well, it may be necessary to include non-standard effects mentioned above as a next step. We leave the theoretical estimation of such effects for future work.

Acknowledgments

We thank Luca Amendola, Hiroyuki Okada, and Tomonori Totani for useful discussions. A. D. F. is supported by JSPS (under the grant No. S12135) and thanks Tokyo University of Science, for the warm hospitality received while part of the project was finalized. S. T. is supported by the Grant-in-Aid for Scientific Research Fund of the Fund of the JSPS No. 24540286 and Scientific Research on Innovative Areas (No. 21111006). S. T. thanks warm hospitalities during his stays in Weihai, Observatorio Nacional in Rio de Janeiro, Passa Quatro, Szczecin, and University of Heidelberg. J. S. A. is supported by CNPq under Grants No. 305857/2010-0 and No. 485669/2011-0 and FAPERJ Grant No. E-26/103.239/2011.

JCAP01(2013)030

References

[1] Supernova Search Team collaboration, A.G. Riess et al., *Observational evidence from supernovae for an accelerating universe and a cosmological constant*, *Astron. J.* **116** (1998) 1009 [astro-ph/9805201] [INSPIRE];
Supernova Cosmology Project collaboration, S. Perlmutter et al., *Measurements of Omega and Lambda from 42 high redshift supernovae*, *Astrophys. J.* **517** (1999) 565 [astro-ph/9812133] [INSPIRE].

[2] WMAP collaboration, D. Spergel et al., *First year Wilkinson Microwave Anisotropy Probe (WMAP) observations: Determination of cosmological parameters*, *Astrophys. J. Suppl.* **148** (2003) 175 [astro-ph/0302209] [INSPIRE].

[3] WMAP collaboration, E. Komatsu et al., *Seven-Year Wilkinson Microwave Anisotropy Probe (WMAP) Observations: Cosmological Interpretation*, *Astrophys. J. Suppl.* **192** (2011) 18 [arXiv:1001.4538] [INSPIRE].

[4] SDSS collaboration, D.J. Eisenstein et al., *Detection of the baryon acoustic peak in the large-scale correlation function of SDSS luminous red galaxies*, *Astrophys. J.* **633** (2005) 560 [astro-ph/0501171] [INSPIRE];
SDSS collaboration, W.J. Percival et al., *Baryon Acoustic Oscillations in the Sloan Digital Sky Survey Data Release 7 Galaxy Sample*, *Mon. Not. Roy. Astron. Soc.* **401** (2010) 2148 [arXiv:0907.1660] [INSPIRE].

[5] S. Weinberg, *The Cosmological Constant Problem*, *Rev. Mod. Phys.* **61** (1989) 1 [INSPIRE].

[6] V. Sahni and A.A. Starobinsky, *The Case for a positive cosmological Lambda term*, *Int. J. Mod. Phys.* **D 9** (2000) 373 [astro-ph/9904398] [INSPIRE].

[7] S.M. Carroll, *The Cosmological constant*, *Living Rev. Rel.* **4** (2001) 1 [astro-ph/0004075] [INSPIRE]. T. Padmanabhan, *Cosmological constant: The Weight of the vacuum*, *Phys. Rept.* **380** (2003) 235 [hep-th/0212290] [INSPIRE];
P. Peebles and B. Ratra, *The Cosmological constant and dark energy*, *Rev. Mod. Phys.* **75** (2003) 559 [astro-ph/0207347] [INSPIRE];
E.J. Copeland, M. Sami and S. Tsujikawa, *Dynamics of dark energy*, *Int. J. Mod. Phys.* **D 15** (2006) 1753 [hep-th/0603057] [INSPIRE];
T.P. Sotiriou and V. Faraoni, *f(R) Theories Of Gravity*, *Rev. Mod. Phys.* **82** (2010) 451 [arXiv:0805.1726] [INSPIRE];
A. De Felice and S. Tsujikawa, *f(R) theories*, *Living Rev. Rel.* **13** (2010) 3 [arXiv:1002.4928] [INSPIRE];
S. Tsujikawa, *Modified gravity models of dark energy*, *Lect. Notes Phys.* **800** (2010) 99 [arXiv:1101.0191] [INSPIRE];
S. Tsujikawa, *Dark energy: investigation and modeling*, arXiv:1004.1493 [INSPIRE].

[8] N. Suzuki, D. Rubin, C. Lidman, G. Aldering, R. Amanullah, et al., *The Hubble Space Telescope Cluster Supernova Survey: V. Improving the Dark Energy Constraints Above $z > 1$ and Building an Early-Type-Hosted Supernova Sample*, *Astrophys. J.* **746** (2012) 85 [arXiv:1105.3470] [INSPIRE].

[9] C. Blake, E. Kazin, F. Beutler, T. Davis, D. Parkinson, et al., *The WiggleZ Dark Energy Survey: mapping the distance-redshift relation with baryon acoustic oscillations*, *Mon. Not. Roy. Astron. Soc.* **418** (2011) 1707 [arXiv:1108.2635] [INSPIRE].

[10] L. Anderson, E. Aubourg, S. Bailey, D. Bizyaev, M. Blanton, et al., *The clustering of galaxies in the SDSS-III Baryon Oscillation Spectroscopic Survey: Baryon Acoustic Oscillations in the Data Release 9 Spectroscopic Galaxy Sample*, *Mon. Not. Roy. Astron. Soc.* **428** (2013) 1036 [arXiv:1203.6594] [INSPIRE].

JCAP01(2013)030

[11] A. De Felice, S. Nesseris and S. Tsujikawa, *Observational constraints on dark energy with a fast varying equation of state*, *JCAP* **05** (2012) 029 [arXiv:1203.6760] [INSPIRE].

[12] Y. Fujii, *Origin of the gravitational constant and particle masses in scale invariant scalar-tensor theory*, *Phys. Rev.* **D 26** (1982) 2580 [INSPIRE];
L. Ford, *Cosmological constant damping by unstable scalar fields*, *Phys. Rev.* **D 35** (1987) 2339 [INSPIRE];
C. Wetterich, *Cosmology and the Fate of Dilatation Symmetry*, *Nucl. Phys.* **B 302** (1988) 668 [INSPIRE];
T. Chiba, N. Sugiyama and T. Nakamura, *Cosmology with x matter*, *Mon. Not. Roy. Astron. Soc.* **289** (1997) L5 [astro-ph/9704199] [INSPIRE];
P.G. Ferreira and M. Joyce, *Structure formation with a selftuning scalar field*, *Phys. Rev. Lett.* **79** (1997) 4740 [astro-ph/9707286] [INSPIRE];
R. Caldwell, R. Dave and P.J. Steinhardt, *Cosmological imprint of an energy component with general equation of state*, *Phys. Rev. Lett.* **80** (1998) 1582 [astro-ph/9708069] [INSPIRE].

[13] C. Armendariz-Picon, T. Damour and V.F. Mukhanov, *k - inflation*, *Phys. Lett.* **B 458** (1999) 209 [hep-th/9904075] [INSPIRE].

[14] T. Chiba, T. Okabe and M. Yamaguchi, *Kinetically driven quintessence*, *Phys. Rev.* **D 62** (2000) 023511 [astro-ph/9912463] [INSPIRE];
C. Armendariz-Picon, V.F. Mukhanov and P.J. Steinhardt, *A Dynamical solution to the problem of a small cosmological constant and late time cosmic acceleration*, *Phys. Rev. Lett.* **85** (2000) 4438 [astro-ph/0004134] [INSPIRE].

[15] S. Capozziello, *Curvature quintessence*, *Int. J. Mod. Phys.* **D 11** (2002) 483 [gr-qc/0201033] [INSPIRE];
S. Capozziello, S. Carloni and A. Troisi, *Quintessence without scalar fields*, *Recent Res. Dev. Astron. Astrophys.* **1** (2003) 625 [astro-ph/0303041] [INSPIRE];
S.M. Carroll, V. Duvvuri, M. Trodden and M.S. Turner, *Is cosmic speed - up due to new gravitational physics?*, *Phys. Rev.* **D 70** (2004) 043528 [astro-ph/0306438] [INSPIRE];
L. Amendola, R. Gannouji, D. Polarski and S. Tsujikawa, *Conditions for the cosmological viability of f(R) dark energy models*, *Phys. Rev.* **D 75** (2007) 083504 [gr-qc/0612180] [INSPIRE];
L. Amendola and S. Tsujikawa, *Phantom crossing, equation-of-state singularities and local gravity constraints in f(R) models*, *Phys. Lett.* **B 660** (2008) 125 [arXiv:0705.0396] [INSPIRE];
W. Hu and I. Sawicki, *Models of f(R) Cosmic Acceleration that Evade Solar-System Tests*, *Phys. Rev.* **D 76** (2007) 064004 [arXiv:0705.1158] [INSPIRE];
A.A. Starobinsky, *Disappearing cosmological constant in f(R) gravity*, *JETP Lett.* **86** (2007) 157 [arXiv:0706.2041] [INSPIRE];
S.A. Appleby and R.A. Battye, *Do consistent $F(R)$ models mimic General Relativity plus Λ?*, *Phys. Lett.* **B 654** (2007) 7 [arXiv:0705.3199] [INSPIRE];
S. Tsujikawa, *Observational signatures of f(R) dark energy models that satisfy cosmological and local gravity constraints*, *Phys. Rev.* **D 77** (2008) 023507 [arXiv:0709.1391] [INSPIRE];
E.V. Linder, *Exponential Gravity*, *Phys. Rev.* **D 80** (2009) 123528 [arXiv:0905.2962] [INSPIRE];
M. Campista, B. Santos, J. Santos and J. Alcaniz, *Cosmological Consequences of Exponential Gravity in Palatini Formalism*, *Phys. Lett.* **B 699** (2011) 320 [arXiv:1012.3943] [INSPIRE];
B. Santos, M. Campista, J. Santos and J. Alcaniz, *Cosmology with Hu-Sawicki gravity in Palatini Formalism*, *Astron. Astrophys.* **548** (2012) A31 [arXiv:1207.2478] [INSPIRE].

[16] SDSS collaboration, M. Tegmark et al., *Cosmological parameters from SDSS and WMAP*, *Phys. Rev.* **D 69** (2004) 103501 [astro-ph/0310723] [INSPIRE];
SDSS collaboration, U. Seljak et al., *Cosmological parameter analysis including SDSS Ly-alpha forest and galaxy bias: Constraints on the primordial spectrum of fluctuations, neutrino mass and dark energy*, *Phys. Rev.* **D 71** (2005) 103515 [astro-ph/0407372] [INSPIRE];

JCAP01(2013)030

SDSS collaboration, M. Tegmark et al., *Cosmological Constraints from the SDSS Luminous Red Galaxies*, *Phys. Rev.* **D 74** (2006) 123507 [astro-ph/0608632] [INSPIRE].

[17] N. Kaiser, *Clustering in real space and in redshift space*, *Mon. Not. Roy. Astron. Soc.* **227** (1987) 1 [INSPIRE].

[18] SDSS collaboration, M. Tegmark et al., *The* $3-D$ *power spectrum of galaxies from the SDSS*, *Astrophys. J.* **606** (2004) 702 [astro-ph/0310725] [INSPIRE].

[19] 2DFGRS collaboration, W.J. Percival et al., *The 2dF Galaxy Redshift Survey: Spherical harmonics analysis of fluctuations in the final catalogue*, *Mon. Not. Roy. Astron. Soc.* **353** (2004) 1201 [astro-ph/0406513] [INSPIRE].

[20] C. Di Porto and L. Amendola, *Observational constraints on the linear fluctuation growth rate*, *Phys. Rev.* **D 77** (2008) 083508 [arXiv:0707.2686] [INSPIRE].

[21] L. Guzzo, M. Pierleoni, B. Meneux, E. Branchini, O.L. Fevre, et al., *A test of the nature of cosmic acceleration using galaxy redshift distortions*, *Nature* **451** (2008) 541 [arXiv:0802.1944] [INSPIRE].

[22] S. Nesseris and L. Perivolaropoulos, *Testing Lambda CDM with the Growth Function delta(a): Current Constraints*, *Phys. Rev.* **D 77** (2008) 023504 [arXiv:0710.1092] [INSPIRE].

[23] U. Alam, V. Sahni and A.A. Starobinsky, *Reconstructing Cosmological Matter Perturbations using Standard Candles and Rulers*, *Astrophys. J.* **704** (2009) 1086 [arXiv:0812.2846] [INSPIRE].

[24] C. Blake, S. Brough, M. Colless, C. Contreras, W. Couch, et al., *The WiggleZ Dark Energy Survey: the growth rate of cosmic structure since redshift z=0.9*, *Mon. Not. Roy. Astron. Soc.* **415** (2011) 2876 [arXiv:1104.2948] [INSPIRE].

[25] L. Samushia, W.J. Percival and A. Raccanelli, *Interpreting large-scale redshift-space distortion measurements*, *Mon. Not. Roy. Astron. Soc.* **420** (2012) 2102 [arXiv:1102.1014] [INSPIRE].

[26] B.A. Reid, L. Samushia, M. White, W.J. Percival, M. Manera, et al., *The clustering of galaxies in the SDSS-III Baryon Oscillation Spectroscopic Survey: measurements of the growth of structure and expansion rate at* $z = 0.57$ *from anisotropic clustering*, arXiv:1203.6641 [INSPIRE].

[27] F. Beutler, C. Blake, M. Colless, D.H. Jones, L. Staveley-Smith, et al., *The 6dF Galaxy Survey:* $z \approx 0$ *measurement of the growth rate and* σ_8, arXiv:1204.4725 [INSPIRE].

[28] E. Jennings, C.M. Baugh, B. Li, G.-B. Zhao and K. Koyama, *Redshift space distortions in f(R) gravity*, arXiv:1205.2698 [INSPIRE].

[29] D. Rapetti, C. Blake, S.W. Allen, A. Mantz, D. Parkinson and F. Beutler, *A combined measurement of cosmic growth and expansion from clusters of galaxies, the CMB and galaxy clustering*, arXiv:1205.4679 [INSPIRE].

[30] L. Samushia, B.A. Reid, M. White, W.J. Percival, A.J. Cuesta, et al., *The Clustering of Galaxies in the SDSS-III DR9 Baryon Oscillation Spectroscopic Survey: Testing Deviations from* Λ *and General Relativity using anisotropic clustering of galaxies*, arXiv:1206.5309 [INSPIRE].

[31] S.A. Appleby and E.V. Linder, *Trial of Galileon gravity by cosmological expansion and growth observations*, *JCAP* **08** (2012) 026 [arXiv:1204.4314] [INSPIRE].

[32] H. Okada, T. Totani and S. Tsujikawa, *Constraints on f(R) theory and Galileons from the latest data of galaxy redshift surveys*, arXiv:1208.4681 [INSPIRE].

[33] S.M. Carroll, I. Sawicki, A. Silvestri and M. Trodden, *Modified-Source Gravity and Cosmological Structure Formation*, *New J. Phys.* **8** (2006) 323 [astro-ph/0607458] [INSPIRE];

JCAP01(2013)030

R. Bean, D. Bernat, L. Pogosian, A. Silvestri and M. Trodden, *Dynamics of Linear Perturbations in f(R) Gravity*, *Phys. Rev.* **D 75** (2007) 064020 [astro-ph/0611321] [INSPIRE];
S. Tsujikawa, *Matter density perturbations and effective gravitational constant in modified gravity models of dark energy*, *Phys. Rev.* **D 76** (2007) 023514 [arXiv:0705.1032] [INSPIRE];
L. Pogosian and A. Silvestri, *The pattern of growth in viable f(R) cosmologies*, *Phys. Rev.* **D 77** (2008) 023503 [*Erratum ibid.* **D 81** (2010) 049901] [arXiv:0709.0296] [INSPIRE];
S. Tsujikawa, R. Gannouji, B. Moraes and D. Polarski, *The dispersion of growth of matter perturbations in f(R) gravity*, *Phys. Rev.* **D 80** (2009) 084044 [arXiv:0908.2669] [INSPIRE].

[34] A. De Felice, R. Kase and S. Tsujikawa, *Matter perturbations in Galileon cosmology*, *Phys. Rev.* **D 83** (2011) 043515 [arXiv:1011.6132] [INSPIRE].

[35] A. De Felice and S. Tsujikawa, *Cosmological constraints on extended Galileon models*, *JCAP* **03** (2012) 025 [arXiv:1112.1774] [INSPIRE].

[36] I. Zlatev, L.-M. Wang and P.J. Steinhardt, *Quintessence, cosmic coincidence and the cosmological constant*, *Phys. Rev. Lett.* **82** (1999) 896 [astro-ph/9807002] [INSPIRE];
P.J. Steinhardt, L.-M. Wang and I. Zlatev, *Cosmological tracking solutions*, *Phys. Rev.* **D 59** (1999) 123504 [astro-ph/9812313] [INSPIRE].

[37] J.M. Bardeen, *Gauge Invariant Cosmological Perturbations*, *Phys. Rev.* **D 22** (1980) 1882 [INSPIRE].

[38] H. Kodama and M. Sasaki, *Cosmological Perturbation Theory*, *Prog. Theor. Phys. Suppl.* **78** (1984) 1 [INSPIRE].

[39] R. Bean and O. Dore, *Probing dark energy perturbations: The Dark energy equation of state and speed of sound as measured by WMAP*, *Phys. Rev.* **D 69** (2004) 083503 [astro-ph/0307100] [INSPIRE].

[40] D. Sapone, M. Kunz and L. Amendola, *Fingerprinting Dark Energy II: weak lensing and galaxy clustering tests*, *Phys. Rev.* **D 82** (2010) 103535 [arXiv:1007.2188] [INSPIRE].

[41] L. Amendola and S. Tsujikawa, *Dark energy — Theory and Observations*, Cambridge University Press U.K. (2010)

[42] B.A. Bassett, S. Tsujikawa and D. Wands, *Inflation dynamics and reheating*, *Rev. Mod. Phys.* **78** (2006) 537 [astro-ph/0507632] [INSPIRE].

[43] J. Garriga and V.F. Mukhanov, *Perturbations in k-inflation*, *Phys. Lett.* **B 458** (1999) 219 [hep-th/9904176] [INSPIRE].

[44] SDSS collaboration, M. Tegmark et al., *Cosmological Constraints from the SDSS Luminous Red Galaxies*, *Phys. Rev.* **D 74** (2006) 123507 [astro-ph/0608632] [INSPIRE].

[45] Y.-S. Song and W.J. Percival, *Reconstructing the history of structure formation using Redshift Distortions*, *JCAP* **10** (2009) 004 [arXiv:0807.0810] [INSPIRE].

[46] M. White, Y.-S. Song and W.J. Percival, *Forecasting Cosmological Constraints from Redshift Surveys*, *Mon. Not. Roy. Astron. Soc.* **397** (2008) 1348 [arXiv:0810.1518] [INSPIRE].

[47] G. Ballesteros and A. Riotto, *Parameterizing the Effect of Dark Energy Perturbations on the Growth of Structures*, *Phys. Lett.* **B 668** (2008) 171 [arXiv:0807.3343] [INSPIRE].

[48] V. Sahni, T.D. Saini, A.A. Starobinsky and U. Alam, *Statefinder: A New geometrical diagnostic of dark energy*, *JETP Lett.* **77** (2003) 201 [astro-ph/0201498] [INSPIRE].

[49] V. Sahni and A. Starobinsky, *Reconstructing Dark Energy*, *Int. J. Mod. Phys.* **D 15** (2006) 2105 [astro-ph/0610026] [INSPIRE].

[50] R. Caldwell and E.V. Linder, *The Limits of quintessence*, *Phys. Rev. Lett.* **95** (2005) 141301 [astro-ph/0505494] [INSPIRE].

JCAP01(2013)030

[51] P. Peebles and B. Ratra, *Cosmology with a Time Variable Cosmological Constant*, *Astrophys. J.* **325** (1988) L17 [INSPIRE];
B. Ratra and P. Peebles, *Cosmological Consequences of a Rolling Homogeneous Scalar Field*, *Phys. Rev.* **D 37** (1988) 3406 [INSPIRE].

[52] T. Chiba, *The Equation of State of Tracker Fields*, *Phys. Rev.* **D 81** (2010) 023515 [arXiv:0909.4365] [INSPIRE].

[53] J.A. Frieman, C.T. Hill, A. Stebbins and I. Waga, *Cosmology with ultralight pseudo Nambu-Goldstone bosons*, *Phys. Rev. Lett.* **75** (1995) 2077 [astro-ph/9505060] [INSPIRE].

[54] S. Dutta and R.J. Scherrer, *Hilltop Quintessence*, *Phys. Rev.* **D 78** (2008) 123525 [arXiv:0809.4441] [INSPIRE].

[55] R.J. Scherrer and A. Sen, *Thawing quintessence with a nearly flat potential*, *Phys. Rev.* **D 77** (2008) 083515 [arXiv:0712.3450] [INSPIRE].

[56] T. Chiba, S. Dutta and R.J. Scherrer, *Slow-roll k-essence*, *Phys. Rev.* **D 80** (2009) 043517 [arXiv:0906.0628] [INSPIRE].

[57] F. Piazza and S. Tsujikawa, *Dilatonic ghost condensate as dark energy*, *JCAP* **07** (2004) 004 [hep-th/0405054] [INSPIRE].

[58] N. Arkani-Hamed, H.-C. Cheng, M.A. Luty and S. Mukohyama, *Ghost condensation and a consistent infrared modification of gravity*, *JHEP* **05** (2004) 074 [hep-th/0312099] [INSPIRE].

[59] L.-M. Wang and P.J. Steinhardt, *Cluster abundance constraints on quintessence models*, *Astrophys. J.* **508** (1998) 483 [astro-ph/9804015] [INSPIRE].

[60] P.J.E. Peebles, *Large-Scale Structure of the Universe,* Princeton University Press U.S.A. (1980)

[61] Y. Gong, M. Ishak and A. Wang, *Growth factor parametrization in curved space*, *Phys. Rev.* **D 80** (2009) 023002 [arXiv:0903.0001] [INSPIRE].

[62] E.V. Linder, *Cosmic growth history and expansion history*, *Phys. Rev.* **D 72** (2005) 043529 [astro-ph/0507263] [INSPIRE];
E.V. Linder and R.N. Cahn, *Parameterized Beyond-Einstein Growth*, *Astropart. Phys.* **28** (2007) 481 [astro-ph/0701317] [INSPIRE].

[63] T. Chiba, A. De Felice and S. Tsujikawa, *Observational Constraints on Quintessence: Thawing, Tracker and Scaling models*, arXiv:1210.3859 [INSPIRE].

JCAP01(2013)030